Neuroscience Research 130 (2018) 56–64

Contents lists available at ScienceDirect

Neuroscience Research

journal homepage: www.elsevier.com/locate/neures

Silencing of FUS in the common marmoset (*Callithrix jacchus*) brain via stereotaxic injection of an adeno-associated virus encoding shRNA

Kuniyuki Endo[a], Shinsuke Ishigaki[a,b,*], Yoshito Masamizu[c,d], Yusuke Fujioka[a], Akiya Watakabe[e], Tetsuo Yamamori[e], Nobuhiko Hatanaka[f], Atsushi Nambu[f], Haruo Okado[g], Masahisa Katsuno[a], Hirohisa Watanabe[h], Masanori Matsuzaki[c,d], Gen Sobue[a,h,i,*]

[a] *Department of Neurology, Nagoya University Graduate School of Medicine, Nagoya, Aichi 466-8550, Japan*
[b] *Department of Therapeutics for Intractable Neurological Disorders, Nagoya University Graduate School of Medicine, Nagoya, Aichi 466-8550, Japan*
[c] *Department of Physiology, Graduate School of Medicine, The University of Tokyo, Bunkyo-ku, Tokyo 113-0033, Japan*
[d] *Division of Brain Circuits, National Institute for Basic Biology, Okazaki, Aichi 444-8585, Japan*
[e] *Laboratory for Molecular Analysis of Higher Brain Function, RIKEN Brain Science Institute, Saitama 351-0198, Japan*
[f] *Division of System Neurophysiology, National Institute for Physiological Sciences, Department of Physiological Sciences, Okazaki, Aichi 444-8585, Japan, and SOKENDAI (The Graduate University for Advanced Studies), Okazaki, Aichi 444-8585, Japan*
[g] *Department of Brain Development and Neural Regeneration, Tokyo Metropolitan Institute of Medical Science, Setagaya-ku, Tokyo 156-8506, Japan*
[h] *Brain and Mind Research Center, Nagoya University, Nagoya, Aichi 466-8550, Japan*
[i] *Research Division of Dementia and Neurodegenerative Disease, Nagoya University Graduate School of Medicine, Nagoya, Aichi 466-8550, Japan*

ARTICLE INFO

Article history:
Received 27 March 2017
Received in revised form 10 August 2017
Accepted 18 August 2017
Available online 24 August 2017

Keywords:
Frontotemporal lobar degeneration
FUS
Common marmoset

ABSTRACT

Fused in sarcoma (FUS) is an RNA binding protein that is involved in frontotemporal lobar degeneration (FTLD) and amyotrophic lateral sclerosis (ALS). To establish the common marmoset (*Callithrix jacchus*) as a model for FTLD, we generated a stereotaxic injection-based marmoset model of FUS-silencing. We designed shRNAs against the marmoset FUS gene and generated an AAV9 virus encoding the most effective shRNA against FUS (shFUS). The AAV encoding shFUS (AAV-shFUS) was introduced into the frontal cortex of young adult marmosets, whereas AAV encoding a control shRNA was injected into the contralateral side. We obtained approximately 70–80% silencing of FUS following AAV-shFUS injection. Interestingly, FUS-silencing provoked a proliferation of astrocytes and microglias. Since FTLD is characterized by various emotional deficits, it would be helpful to establish a marmoset model of FUS-silencing in various brain tissues for investigating the pathomechanism of higher cognitive and behavioral dysfunction.

1. Introduction

Frontotemporal lobar degeneration (FTLD) is a general term to describe the pathological syndrome characterized by selective involvement of the frontal and/or temporal lobes with relative preservation of the posterior lobe. FTLD is thought to be equivalent to frontotemporal dementia (FTD), a clinical term that includes three prototypic syndromes: behavioral variant frontotemporal dementia (bvFTD), progressive nonfluent aphasia (PNFA), and semantic dementia (SD) (Neary et al., 1998). These syndromes are characterized by behavioral changes, language impairment, or cognitive decline. FTLD is now known as a broader spectrum syndrome that includes tauopathies such as progressive supranuclear palsy (PSP) and corticobasal syndrome (CBS), which are characterized by an accumulation of phosphorylated tau, and FTD with motor neuron disease (FTD-MND/FTD-ALS) characterized by ubiquitin-positive inclusions of TAR DNA-binding protein of 43 kDa (TDP-43) or fused in sarcoma (FUS) (Kertesz et al., 2005; Neumann et al., 2009; Neumann et al., 2006; Seelaar et al., 2011).

FUS is an RNA-binding protein that regulates aspects of RNA metabolism including gene transcription, RNA splicing, and mRNA transport (Lagier-Tourenne and Cleveland, 2009; Strong and Volkening, 2011). Mislocalization of FUS from the nucleus to the

Abbreviations: FTLD, frontotemporal lobar degeneration; ALS, amyotrophic lateral sclerosis; FUS, fused in sarcoma; AAV, adeno-associated virus.

* Corresponding authors at: Department of Neurology, Nagoya University Graduate School of Medicine, Nagoya, Aichi 466-8550, Japan.
E-mail addresses: ishigaki-ns@umin.net (S. Ishigaki), sobueg@med.nagoya-u.ac.jp (G. Sobue).

https://doi.org/10.1016/j.neures.2017.08.006
0168-0102/

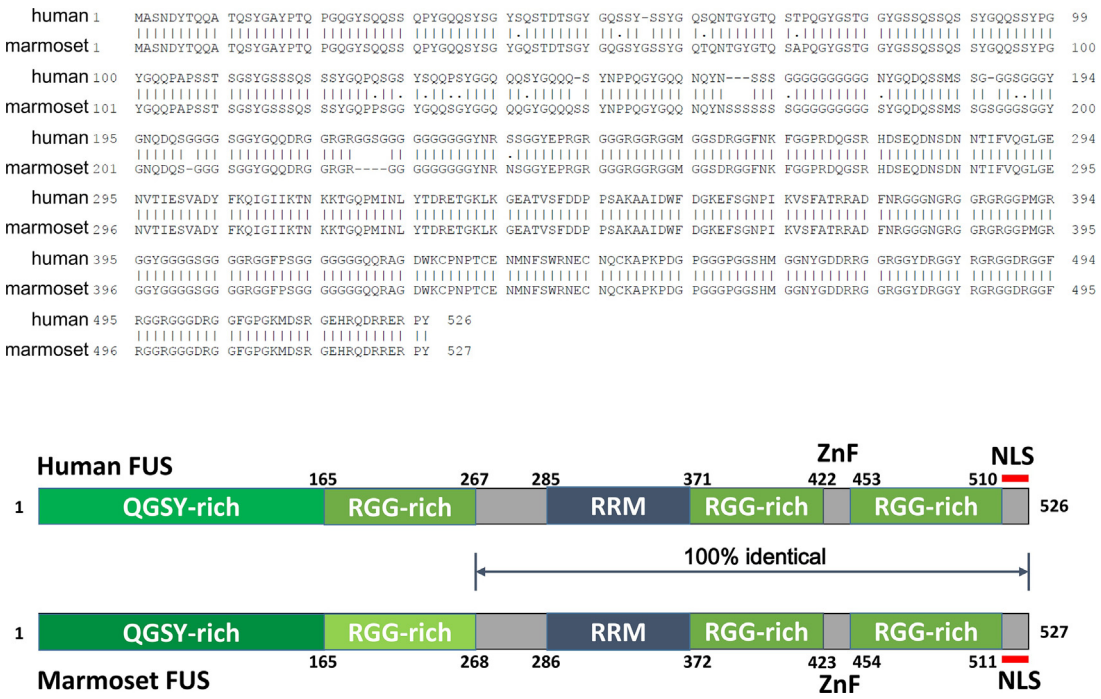

Fig. 1. Comparison of the human and marmoset FUS amino acid sequences.
The complete sequences of the human and marmoset FUS proteins are shown in the upper panel. The Genbank/EBI accession is LC193721. A comparison of the structural features of the human and marmoset FUS is shown in the lower panel. The C-terminal region of FUS is completely conserved between human and marmoset.

cytoplasm in affected neurons suggests that the loss of nuclear FUS is causal for neurodegeneration. Although loss-of-FUS-function in motor neurons might not contribute to motor neuron degeneration (Scekic-Zahirovic et al., 2016; Sharma et al., 2016), it has been shown that loss of FUS leads to neuronal cell death in *Drosophila* and zebrafish (Kabashi et al., 2011; Wang et al., 2011). Furthermore, we have recently reported that the introduction of an adeno-associated virus (AAV)-shRNA targeting FUS in the hippocampus of mice reduced FUS levels and resulted in FTLD-like behaviors including the development of emotional disorders (Ishigaki et al., 2017; Udagawa et al., 2015). These results suggest that loss of FUS in cerebral neurons can contribute to neuronal dysfunction and neurodegeneration in FTLD. While FUS-silenced mice are useful animal models for FTLD, the utility of rodent models for investigating higher behavioral and cognitive impairments such as social abnormality, a major clinical hallmark of FTLD, is limited. Scientific interest in the common marmoset (*Callithrix jacchus*) as a model for investigating social behaviors comparable to those of humans has gained traction given their complex social and cognitive behaviors and similar core brain architecture (Miller et al., 2016). Here, we developed an adeno-associated virus (AAV)-based system for FUS knockdown in adult common marmosets.

2. Material and methods

2.1. Cloning of marmoset FUS gene

Total RNA samples prepared from marmoset brain specimens were reverse transcribed using Superscript IV (Invitrogen). A search of the Ensembl genome database facilitated the development of primers to the 5′-UTR and the terminal end of the coding sequence (CDS) of the marmoset FUS homologue. This gene fragment was amplified by PCR.

Table 1
si/shRNAs used in this study.

si/shRNA Name	Target Sequence
marmoset FUS1	GATTGGTATTATTAAGACA
marmoset FUS2	GATTATACTCAACAAGCAA
marmoset FUS3	GGGCGAGAATGTTACAATT
Cont	AATTCTCCGAACGTGTCACGT

2.2. Lentivirus vector preparation for HEK293T cells expressing EGFP-marmoset FUS

We used a lentiviral system that expresses EGFP fused with the marmoset FUS. Briefly, the CDS portion of marmoset FUS was sub-cloned into an entry vector containing the EGFP sequence (pENTR4-GFP2), and then recombined into a lentiviral expression vector (pLenti-CMV, 705-1). Lentiviral particles were produced in HEK293T cells by transfection using Lipofectamine 2000 (Invitrogen). The lentiviral-containing supernatant was collected 48 h after transfection, and stored at −80 °C. Details on the lentivirus system have been described previously (Campeau et al., 2009). HEK293T cells infected with the lentivirus expressing EGFP-marmoset FUS were used to screen si/shRNAs for the marmoset FUS.

2.3. Screening for shRNAs targeting the marmoset FUS

Candidate siRNAs were developed using the website-based software, i-Score Designer (http://www.med.nagoya-u.ac.jp/neurogenetics/i_Score/i_score.html) and then transfected into HEK293T cells stably expressing EGFP-marmoset FUS (Table 1). The intensity of EGFP fluorescence was determined using fluorescence microscopy, whereas the expression level of marmoset FUS was measured by western blot. The most effective siRNA (marmoset FUS1) was selected and used to generate an AAV-shRNA targeting the marmoset FUS.

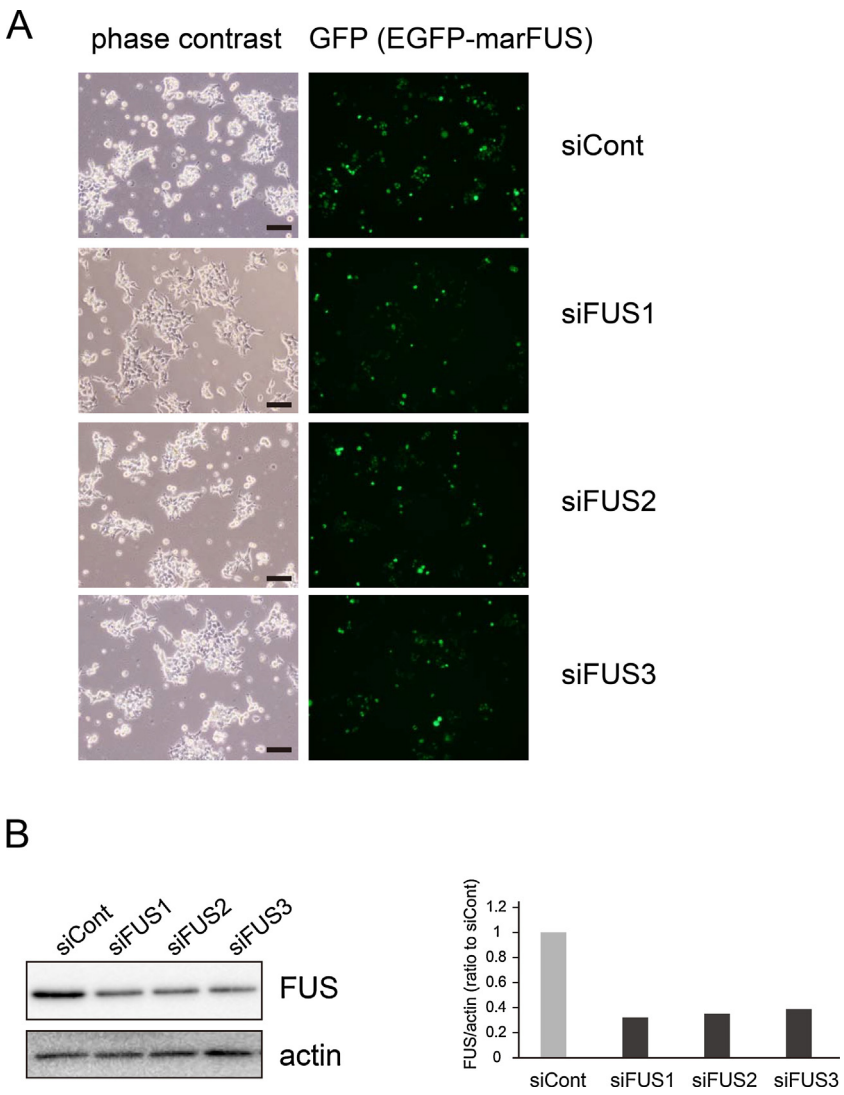

Fig. 2. Screening of siRNAs targeting marmoset FUS.
A. HEK293T cells expressing EGFP-tagged marmoset FUS were imaged using a fluorescent microscope following treatment with candidate siRNAs targeting the marmoset FUS. Scale bars, 100 μm. The siRNA sequences are shown in Table 1. B. Protein extracts from HEK293T cells expressing the EGFP-tagged marmoset FUS were immunoblotted with an anti-FUS antibody following treatment with candidate siRNAs targeting the marmoset FUS. FUS-associated signal intensities were measured.

2.4. AAV production

The AAV-s1/shRNA-marmoset FUS virus has an AAV9 serotype backbone that uses an H1 promoter to express an shRNA targeting the marmoset FUS gene and a CAG promoter that drives EGFP expression, which allows for visual detection of cells expressing the shRNA (Noro et al., 2004). Production and purification of AAVs were performed as described previously (Ishigaki et al., 2017; Okada et al., 2009). Titers of the viral stocks were determined by qPCR.

2.5. Stereotaxic injection of an AAV into the marmoset cortex

Animal experiments were performed in accordance with the National Institutes of Health Guide for the Care and Use of Laboratory Animals and under the approval of the Institutional Animal Care and Use Committee of the National Institutes of Natural Sciences (Okazaki, Japan). AAVs were injected into two female marmosets (57-month and 73-month old) as described previously (Masamizu et al., 2011; Masamizu et al., 2014). An antibiotic, Cefovecin sodium (Convenia®-Pfizer, 14 mg/kg) and an anti-inflammatory agent, Carprofen (Rimadyl®-Pfizer, 3.75 mg/kg) were administered intramuscularly. Acetated Ringer's solution (Solyugen F®-KYOWA CritiCare, 10 ml) including riboflavin phosphate sodium (Bisulase®-TOA EIYO, 20 μl) was administered subcutaneously. The marmoset was then placed in a stereotaxic apparatus (SR-5C; Narishige, Tokyo, Japan) under anesthesia, which was maintained using inhaled isoflurane (1.5–4.0% in oxygen). The marmoset's condition was assessed by continuously monitoring pulse oxygen (SpO_2), heart rate, and rectal temperature. Four small craniotomies (1–2 mm in diameter) were made over the bilateral parietal lobe (Yuasa et al., 2010), and the underlying dura was slit to allow penetration of a pulled glass pipet. Before virus injection, the pulled glass pipette (broken and beveled to 70-μm outer diameter; Sutter Instruments, CA, USA) and a 5-μl Hamilton syringe were back-filled with mineral oil (Nacalai Tesque, Inc., Kyoto, Japan) and front-loaded with virus solution. The pipette was inserted vertically approximately 500 μm ventral from the brain surface. Small volume aliquots (1 μl) of AAV carrying shRNA targeting marmoset FUS (shFUS) at concentrations of 5.0×10^{13} VG/ml and 5.0×10^{12} VG/ml were injected into two separate portions of the first marmoset (57-

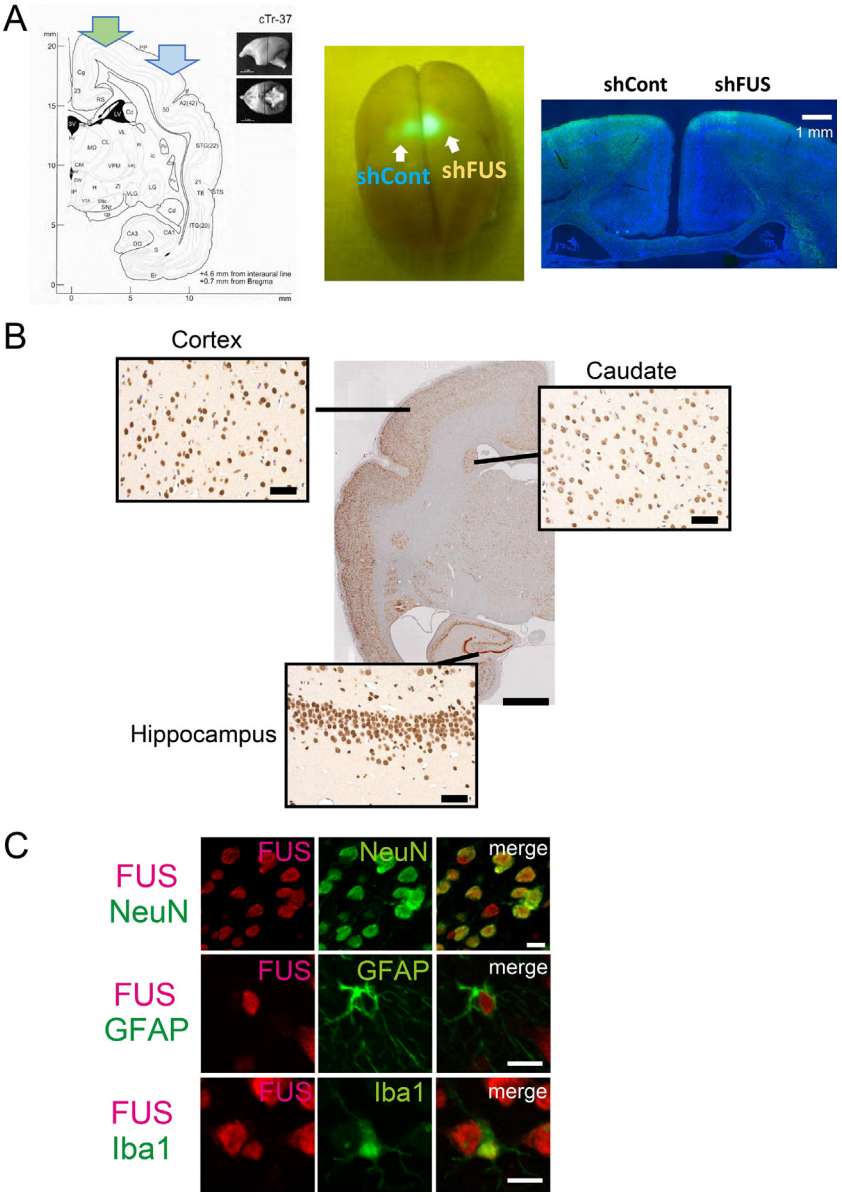

Fig. 3. Stereotaxic injection of AAV into the cortex and the distribution of FUS in the marmoset brain.
A. AAV carrying shRNA targeting marmoset FUS (shFUS) at different concentrations was injected into the two separate portions of the right cerebral cortex of an adult marmoset. A green arrow indicates the injection site of the higher virus titer (1 μl of 5.0×10^{13} VG/ml), whereas a light blue arrow indicates the injection site of the lower virus titer (1 μl of 5.0×10^{12} VG/ml) (left image). Similarly, AAV carrying the control shRNA (shCont) at different concentrations was also injected into the two separate portions of the left cerebral cortex of the same animal (middle image). The EGFP signals were distributed to an area 1 mm in radius from the center of the high viral titer injection site (right image). B. Paraffin embedded brain sections were stained with an anti-FUS antibody using a DAB peroxidase substrate. High magnification images of the cortex, caudate, and hippocampus are shown. Scale bar, 2 mm for the low magnification image, 20 μm for high magnification images. C. Immunofluorescent images of the cortex stained with cell-specific markers. The sections were stained with anti-FUS and anti-NeuN (top), anti-GFAP (middle), or anti-Iba1 (bottom) antibodies, respectively. Scale bars, 10 μm.

month old female) right cerebral cortex. Similarly, 1-μl aliquots (5.0×10^{13} VG/ml and 5.0×10^{12} VG/ml) of AAV carrying control shRNA (shCont) were injected into two separate portions of the left cerebral cortex of the same animal. We repeated the injection experiments using a second marmoset (73-month old female). In this second set of injections, only a single concentration (5.0×10^{13} VG/ml) was injected and the shFUS AAV was injected into the left cerebral cortex, whereas the shCont AAV was injected into the right cerebral cortex of the same animal. Samples were injected at a flow rate of 0.1 μl/min with a syringe pump (KDS310; KD Scientific, MA, USA). After injection, the pipette was maintained in place for an additional 5 min before being slowly withdrawn.

2.6. Preparation of brain slices and immunohistochemistry/immunofluorescent analysis

Brain slices were prepared from the first and second marmosets 6 and 8 weeks after AAV injection, respectively. Perfusion fixation was performed under deep anesthesia with sodium pentobarbital (40 mg/kg, i.p., Sumitomo Dainippon Pharma Co., Ltd., Osaka, Japan) as described previously (Sadakane et al., 2015). Injected marmosets were decapitated under deep anesthesia using sodium pentobarbital (Sumitomo Dainippon Pharma Co., Ltd., Osaka, Japan). The brain was quickly removed after perfusion through the left cardiac ventricle of the marmoset with 500 ml normal saline, followed by

500 ml of a 4% paraformaldehyde (PFA) fixative in phosphate buffer solution (Wako Pure Chemical Industries, Ltd., Osaka, Japan). Tissues were post-fixed for a week in 4% PFA and then processed for paraffin embedding. Tissues were de-paraffinized as 3-μm thick tissue sections and dehydrated with alcohol. Sections were initially microwaved for 5 min in 50 mM citrate buffer (pH 6.0), treated with TNB blocking buffer (PerkinElmer Japan Co., Ltd., Kanagawa, Japan) and then incubated overnight with mouse anti-FUS monoclonal antibody (1:1000, 4H11:sc-47711; Santa Cruz Biotechnology, Inc., TX, USA), rabbit anti-FUS polyclonal antibody (1:5000, A300-293A; Bethyl Laboratories, Inc., TX, USA), rabbit anti-Green Fluorescent Protein (GFP) polyclonal antibody (1:500; Medical and Biologocal Laboratories, Co., Ltd., Nagoya, Japan), mouse anti-neuronal nuclei (NeuN) monoclonal antibody (1:500, MAB377; Merck Millipore, Co., Darmstadt, Germany), mouse anti-GFAP monoclonal antibody (1:1000, EB4, Enzo), or rabbit anti-Iba1 polyclonal antibody (1:500; Wako Pure Chemical Industries, Ltd., Osaka, Japan). Sections were then incubated with the indicated secondary antibody for 60 min. After washing, sections were sealed with Mount-Quick® (Cosmo Bio, Co., Ltd., Tokyo, Japan) for immunohistochemistry or 4′,6-diamidino-2-phenylindole (DAPI) Fluoromount-G® (SouthernBiotech, AL, USA) for immunofluorescent analysis. Brain slices were then imaged with a laser confocal microscope (LSM710; Zeiss, Oberkochen, Germany).

2.7. Quantitative image analysis

To quantify the level of FUS in the marmoset brain, the signal intensities of FUS in EGFP positive cells (n = 10 for each) were measured and the mean signal intensities were compared between shFUS and shCont-injected lesions using imaging software (ZEN 2012; Zeiss, Oberkochen, Germany). Similarly, the expression levels of GFAP, Iba1, and NeuN in each imaging field (n = 10 for each) of the marmoset brain were quantified using a digital imaging analyzer (BZ-H3C, Keyence, Osaka, Japan). The mean number of positive cells was counted and the mean signal intensities were compared between the shFUS and shCont-injected lesions.

2.8. Statistical analysis

Statistical analyses were performed using JMP 13 (SAS Institute, NC, USA). Two groups were compared by the unpaired *t*-tests as described in the Figure legends, and statistical significance was set to $P < 0.05$. The data was expressed as mean ± SD.

3. Results

3.1. Cloning of the marmoset FUS gene

We obtained partial sequences of the marmoset FUS mRNA from the Ensembl database and designed primers spanning the complete FUS gene CDS. RT-PCR using the specific primers with cDNA generated from marmoset cortex total RNA yielded a specific product of 1.6 kbp that included the complete open reading frame (ORF) of the marmoset FUS (Fig. 1, Gen Bank/EBI No. LC193721). A BLASTn search revealed that the identified marmoset FUS gene mapped to chromosome 12 and is 94% identical to the human FUS gene (Fig. S1). A BLASTp search indicated that the amino acid sequence of the marmoset FUS is 90% identical to the human protein. Furthermore, the C-terminal region of the FUS protein where many of disease-associated mutations have been identified (Lagier-Tourenne et al., 2010) is 100% identical between human and marmoset (Fig. 1).

3.2. Selection of si/shRNA targeting marmoset FUS

We next sub-cloned the marmoset FUS ORF into a lentiviral vector to generate a chimeric protein with EGFP fused to the marmoset FUS N-terminus. HEK293T cells were infected with the EGFP-marmoset-FUS expressing lentivirus and a single clone stably expressing the construct was selected (Fig. 2A). Using this cell line, siRNAs targeting marmoset FUS were screened by measuring EGFP fluorescence and the protein levels of marmoset FUS (Fig. 2B). Based on this screening approach, we determined that siFUS1 was the most effective siRNA for the marmoset FUS.

3.3. Stereotaxic injection of AAV expressing shRNA targeting marmoset FUS

One-μl of 5.0×10^{13} VG/ml and of 5.0×10^{12} VG/ml of AAV shFUS were injected into two separate portions of the right cerebral cortex, and 1-μl of 5.0×10^{13} VG/ml and of 5.0×10^{12} VG/ml of AAV shCont were injected into two separate portions of the left cerebral cortex in the first animal (Fig. 3A, left). No apparent motor deficits were observed in the animal after AAV injection. We observed EGFP signals on the surface of the brain (Fig. 3A, middle) that were distributed within a 1 mm radius from the center of the higher virus titer injection (Fig. 3A, right).

3.4. Immunohistochemistry and immunofluorescent analysis of FUS expression in the marmoset brain

Using paraffin embedded brain sections stained with an anti-FUS antibody, we confirmed that FUS was ubiquitously expressed in the marmoset brain including the cortex, caudate, and hippocampus (Fig. 3B). In addition, FUS was positively stained in all cell types including neurons, astrocytes, and microglia cells (Fig. 3C).

3.5. Immunofluorescent analysis of the FUS-silenced marmoset brain

The paraffin embedded brain sections were stained with anti-GFP and anti-FUS antibodies. FUS signals were suppressed in the EGFP-positive lesion where the high titer AAV-shFUS (5.0×10^{13} VG/ml) was injected (the first and second animals). In contrast, no FUS signal suppression was observed in the left cortex EGFP-positive lesion in which AAV shCont of the same titer concentration was introduced (Fig. 4A). The lesion injected with the lower titer AAV-shFUS (5.0×10^{12} VG/ml) did not exhibit the decrease in FUS signals in the EGFP-positive neurons (the first animal). Using confocal microscopy, we quantified levels of the FUS signal in EGFP-positive cells in the cortex. We obtained ~80% FUS knockdown in shFUS-introduced cells compared to shCont-introduced cells in the first and second marmosets (Fig. 4B). FUS signals in the nucleus were reduced by shFUS in all cell types including neurons (NeuN-positive cells), astrocytes (GFAP-positive cells), and microglias (Iba1-positive cells) (Fig. 4C). There was no apparent neuronal cell loss associated with FUS-silencing. Next, we stained with anti-GFAP and anti-Iba1 antibodies to investigate the immunological response to FUS-silencing. Interestingly, more GFAP positive and Iba1 positive cells were observed in the shFUS-introduced cortex than in the shCont-introduced cortex (Fig. 5A). The signal intensities of GFAP and Iba1 were measured and the signal levels and the cell counts for each marker were quantified (the first and second animals). Compared to the control-injection, FUS-silencing significantly increased the number of astrocytes and microglias (Fig. 5B) but had no effect on neurons (data not shown).

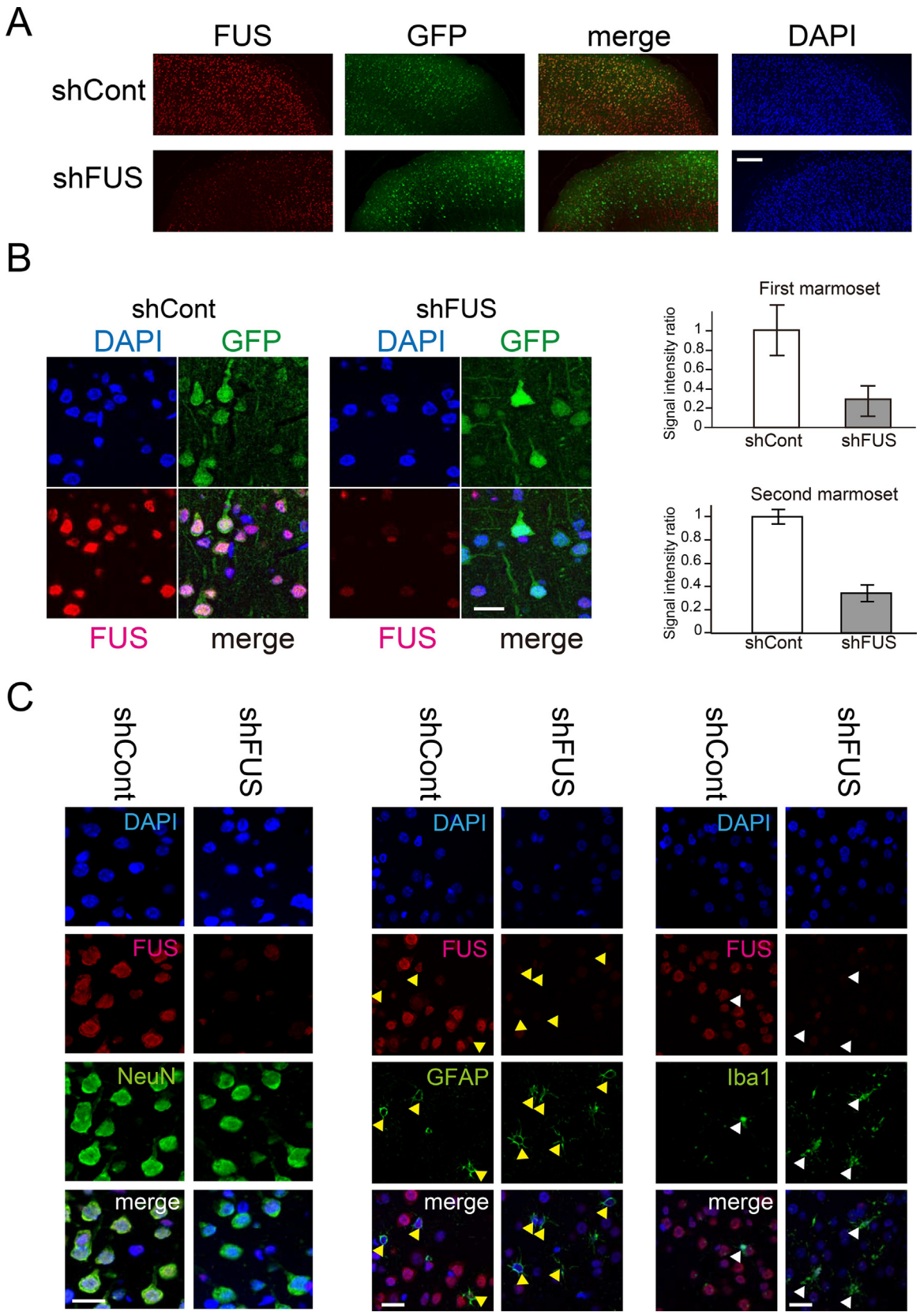

Fig. 4. Stereotaxic injection into the cortex of AAV-shFUS successfully silences FUS expressions in the cortex.
A. Paraffin embedded brain sections were stained with anti-GFP (green) and anti-FUS (red) antibodies. Scale bar, 200 μm. B. The signal levels of FUS in EGFP-positive neurons in the cortex were measured and quantified using a confocal microscope (left images). Scale bar, 20 μm. The quantified signals levels are shown as a graph (the first marmoset in right upper graph and the second marmoset in right lower graph). Data are mean ± SD. C. Immunofluorescent images of the cortex stained with cell-specific markers. The sections injected with shCont or shFUS were stained with anti-FUS and anti-NeuN (left), anti-GFAP (middle), or anti-Iba1 (right) antibodies, respectively. Yellow and white arrowheads indicate nuclei with FUS signals in GFAP and Iba1-positive cells, respectively. Scale bars, 20 μm.

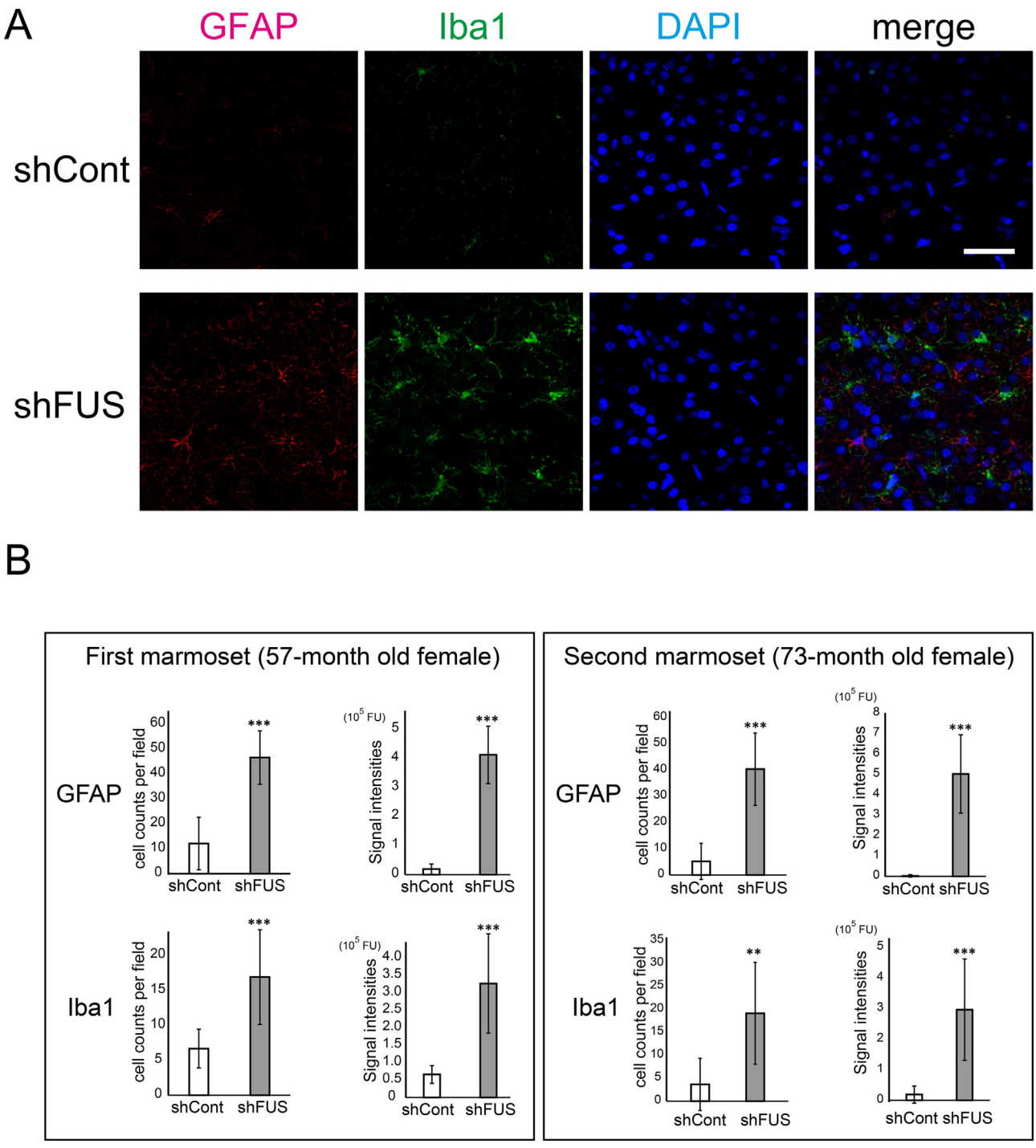

Fig. 5. Higher immunological response is observed in the shFUS-injected cortex than the shCont-injected cortex.
A. Paraffin embedded brain sections were immunostained with anti-Iba1 (green) and anti-GFAP (red) antibodies to investigate the effect of FUS-silencing on the immunological response. Scale bar, 50 μm. B. The signal intensities of GFAP- or Iba1-positive cell counts were quantified (the first marmoset in the left panel and the second marmoset in the right panel). ***P < 0.001, N.S. denotes not significant. Data are mean ± SD.

4. Discussion

Redistribution of FUS from the nucleus to the cytoplasm implies that the loss of nuclear FUS is causal for FUS-associated FTLD/ALS. Indeed, loss of FUS leads to neuronal cell death in *Drosophila* and zebrafish (Kabashi et al., 2011; Wang et al., 2011). Although the previous reports suggested that loss-of-FUS-function in motor neurons might not contribute to motor neuron degeneration in ALS (Scekic-Zahirovic et al., 2016; Sharma et al., 2016), our recent studies show that loss-of-FUS-function in cerebral neurons might contribute to neuronal dysfunction and neurodegeneration in FTLD (Ishigaki et al., 2017; Udagawa et al., 2015).

In this study, the common marmoset FUS gene was fully cloned based on the Ensembl database sequence. It Exhibits 94% nucleotide identity and 90% amino acid identity with human FUS, and has conserved protein motifs such as RRMs. Immunohistochemistry analysis (Fig. 3) showed that marmoset FUS, like its mouse and human homologs, is localized in neurons and glial cells of the brain.

The injected AAV was distributed to an area 1 mm in radius from the center of the injection site, which is comparable in size to that seen following injection in the mouse brain. The 80% reduction in FUS signals verified the efficacy of our shFUS AAV for targeting marmoset FUS and was consistent with the mouse version of shFUS AAVs used in our previous studies (Ishigaki et al., 2017; Udagawa et al., 2015).

The expression pattern of FUS in the marmoset cortex was observed ubiquitously in the marmoset brain and in all cell types including neurons, astrocytes, and microglia cells (Fig. 3). It is notable that a proliferation of glial cells was observed in the shFUS cortex compared to the shCont cortex, which did not exhibit neuronal loss (Fig. 5). Glial activation is one of the major histopathological features in various neurodegeneration disorders including ALS/FTLD (Philips and Robberecht, 2011). Although a glial reaction was reported in a FUS transgenic rat model (Huang et al., 2011), glial activation observed in our shFUS marmoset occurred only 8 weeks post-injection without neuronal loss. These results suggest that the mechanism might be different from one generated in a non-cell autonomous fashion that has accompanying neuronal loss. We previously reported that many immunologically associated genes were differentially expressed in FUS-silenced primary glial cells, indicating that loss of FUS could directly cause glial cell activation (Fujioka et al., 2013). Since we observed that AAV9 injection itself caused a certain level of inflammation in the mouse brain that masked differences in inflammation between shFUS and shCont (data not shown), it would be meaningful to use the marmoset brain for investigation of the precise role of FUS in glial activation.

The common marmoset is better suited than rodents or other simple vertebrate models for studying higher cognitive behaviors. We recapitulated portions of these phenotypes by establishing a mouse model with hippocampus-specific silencing of FUS (Ishigaki et al., 2017; Udagawa et al., 2015); however, it would be helpful to establish a marmoset model of FUS-silencing in various brain tissues including hippocampus or caudate for a more detailed interpretation of the neuronal pathways affected by the FTLD pathomechanism.

5. Conclusions

We identified the CDS of FUS in the common marmoset and demonstrated ubiquitous distribution in the brain. We successfully silenced FUS in the brain of the common marmoset using an adeno-associated virus (AAV)-expressing shRNA targeting marmoset FUS. We observed more pronounced inflammation after injection of the FUS AAV-shRNA than the control.

Formatting of funding sources

This study represents the results of Brain/MINDS of the Ministry of Education, Culture, Sports, Science and Technology of Japan (MEXT) and the Japan Agency for Medical Research and Development (AMED). A part of this study represents the results of the “Integrated Research on Depression, Dementia and Development Disorders” and the “Construction of System for Spread of Primate Model Animals” projects carried out under the Strategic Research Program for Brain Sciences by AMED. It was also supported by Grant-in-Aid for Scientific Research on Innovative Areas, “Brain Protein Aging and Dementia control” and “Non-linear Neurooscillology” from MEXT.

Acknowledgements

We thank A. Miwa and S. Hirai for technical support in AAV production.

Appendix A. Supplementary data

Supplementary data associated with this article can be found, in the online version, at http://dx.doi.org/10.1016/j.neures.2017.08.006.

References

Campeau, E., Ruhl, V.E., Rodier, F., Smith, C.L., Rahmberg, B.L., Fuss, J.O., Campisi, J., Yaswen, P., Cooper, P.K., Kaufman, P.D., 2009. A versatile viral system for expression and depletion of proteins in mammalian cells. PLoS One 4, e6529.

Fujioka, Y., Ishigaki, S., Masuda, A., Iguchi, Y., Udagawa, T., Watanabe, H., Katsuno, M., Ohno, K., Sobue, G., 2013. FUS-regulated region- and cell-type-specific transcriptome is associated with cell selectivity in ALS/FTLD. Sci. Rep. 3, 2388.

Huang, C., Zhou, H., Tong, J., Chen, H., Liu, Y.J., Wang, D., Wei, X., Xia, X.G., 2011. FUS transgenic rats develop the phenotypes of amyotrophic lateral sclerosis and frontotemporal lobar degeneration. PLoS Genet. 7, e1002011.

Ishigaki, S., Fujioka, Y., Okada, Y., Riku, Y., Udagawa, T., Honda, D., Yokoi, S., Endo, K., Ikenaka, K., Takagi, S., Iguchi, Y., Sahara, N., Takashima, A., Okano, H., Yoshida, M., Warita, H., Aoki, M., Watanabe, H., Okado, H., Katsuno, M., Sobue, G., 2017. Altered tau isoform ratio caused by loss of FUS and SFPQ function leads to FTLD-like phenotypes. Cell Rep. 18, 1118–1131.

Kabashi, E., Bercier, V., Lissouba, A., Liao, M., Brustein, E., Rouleau, G.A., Drapeau, P., 2011. FUS and TARDBP but not SOD1 interact in genetic models of amyotrophic lateral sclerosis. PLoS Genet. 7, e1002214.

Kertesz, A., McMonagle, P., Blair, M., Davidson, W., Munoz, D.G., 2005. The evolution and pathology of frontotemporal dementia. Brain: J. Neurol. 128, 1996–2005.

Lagier-Tourenne, C., Cleveland, D.W., 2009. Rethinking ALS: the FUS about TDP-43. Cell 136, 1001–1004.

Lagier-Tourenne, C., Polymenidou, M., Cleveland, D.W., 2010. TDP-43 and FUS/TLS: emerging roles in RNA processing and neurodegeneration. Hum. Mol. Genet. 19, R46–64.

Masamizu, Y., Okada, T., Kawasaki, K., Ishibashi, H., Yuasa, S., Takeda, S., Hasegawa, I., Nakahara, K., 2011. Local and retrograde gene transfer into primate neuronal pathways via adeno-associated virus serotype 8 and 9. Neuroscience 193, 249–258.

Masamizu, Y., Tanaka, Y.R., Tanaka, Y.H., Hira, R., Ohkubo, F., Kitamura, K., Isomura, Y., Okada, T., Matsuzaki, M., 2014. Two distinct layer-specific dynamics of cortical ensembles during learning of a motor task. Nat. Neurosci. 17, 987–994.

Miller, C.T., Freiwald, W.A., Leopold, D.A., Mitchell, J.F., Silva, A.C., Wang, X., 2016. Marmosets: a neuroscientific model of human social behavior. Neuron 90, 219–233.

Neary, D., Snowden, J.S., Gustafson, L., Passant, U., Stuss, D., Black, S., Freedman, M., Kertesz, A., Robert, P.H., Albert, M., Boone, K., Miller, B.L., Cummings, J., Benson, D.F., 1998. Frontotemporal lobar degeneration: a consensus on clinical diagnostic criteria. Neurology 51, 1546–1554.

Neumann, M., Sampathu, D.M., Kwong, L.K., Truax, A.C., Micsenyi, M.C., Chou, T.T., Bruce, J., Schuck, T., Grossman, M., Clark, C.M., McCluskey, L.F., Miller, B.L., Masliah, E., Mackenzie, I.R., Feldman, H., Feiden, W., Kretzschmar, H.A., Trojanowski, J.Q., Lee, V.M., 2006. Ubiquitinated TDP-43 in frontotemporal lobar degeneration and amyotrophic lateral sclerosis. Science 314, 130–133.

Neumann, M., Rademakers, R., Roeber, S., Baker, M., Kretzschmar, H.A., Mackenzie, I.R., 2009. A new subtype of frontotemporal lobar degeneration with FUS pathology. Brain: J. Neurol. 132, 2922–2931.

Noro, T., Miyake, K., Suzuki-Miyake, N., Igarashi, T., Uchida, E., Misawa, T., Yamazaki, Y., Shimada, T., 2004. Adeno-associated viral vector-mediated expression of endostatin inhibits tumor growth and metastasis in an orthotropic pancreatic cancer model in hamsters. Cancer Res. 64, 7486–7490.

Okada, T., Nonaka-Sarukawa, M., Uchibori, R., Kinoshita, K., Hayashita-Kinoh, H., Nitahara-Kasahara, Y., Takeda, S., Ozawa, K., 2009. Scalable purification of adeno-associated virus serotype 1 (AAV1) and AAV8 vectors, using dual ion-exchange adsorptive membranes. Hum. Gene Ther. 20, 1013–1021.

Philips, T., Robberecht, W., 2011. Neuroinflammation in amyotrophic lateral sclerosis: role of glial activation in motor neuron disease. Lancet Neurol. 10, 253–263.

Sadakane, O., Masamizu, Y., Watakabe, A., Terada, S., Ohtsuka, M., Takaji, M., Mizukami, H., Ozawa, K., Kawasaki, H., Matsuzaki, M., Yamamori, T., 2015. Long-Term two-Photon calcium imaging of neuronal populations with subcellular resolution in adult non-human primates. Cell Rep. 13, 1989–1999.

Scekic-Zahirovic, J., Sendscheid, O., El Oussini, H., Jambeau, M., Sun, Y., Mersmann, S., Wagner, M., Dieterle, S., Sinniger, J., Dirrig-Grosch, S., Drenner, K., Birling, M.C., Qiu, J., Zhou, Y., Li, H., Fu, X.D., Rouaux, C., Shelkovnikova, T., Witting, A., Ludolph, A.C., Kiefer, F., Storkebaum, E., Lagier-Tourenne, C., Dupuis, L., 2016. Toxic gain of function from mutant FUS protein is crucial to trigger cell autonomous motor neuron loss. EMBO J. 35, 1077–1097.

Seelaar, H., Rohrer, J.D., Pijnenburg, Y.A., Fox, N.C., van Swieten, J.C., 2011. Clinical, genetic and pathological heterogeneity of frontotemporal dementia: a review. J. Neurol. Neurosurg. Psychiatry 82, 476–486.

Sharma, A., Lyashchenko, A.K., Lu, L., Nasrabady, S.E., Elmaleh, M., Mendelsohn, M., Nemes, A., Tapia, J.C., Mentis, G.Z., Shneider, N.A., 2016. ALS-associated mutant FUS induces selective motor neuron degeneration through toxic gain of function. Nat. Commun. 7, 10465.

Strong, M.J., Volkening, K., 2011. TDP-43 and FUS/TLS: sending a complex message about messenger RNA in amyotrophic lateral sclerosis? FEBS J. 278, 3569–3577.

Udagawa, T., Fujioka, Y., Tanaka, M., Honda, D., Yokoi, S., Riku, Y., Ibi, D., Nagai, T., Yamada, K., Watanabe, H., Katsuno, M., Inada, T., Ohno, K., Sokabe, M., Okado, H., Ishigaki, S., Sobue, G., 2015. FUS regulates AMPA receptor function and FTLD/ALS-associated behaviour via GluA1 mRNA stabilization. Nat. Commun. 6, 7098.

Wang, J.W., Brent, J.R., Tomlinson, A., Shneider, N.A., McCabe, B.D., 2011. The ALS-associated proteins FUS and TDP-43 function together to affect Drosophila locomotion and life span. J. Clin. Invest. 121, 4118–4126.

Yuasa, S., Nakamura, K., Kohsaka, S., 2010. Stereotaxic Atlas of the Marmoset Brain With Immunohistochemical Architecture and MR Images. Igaku Shoin, Tokyo.